THE JOURNAL OF BIOLOGICAL CHEMISTRY
Vol. 277, No. 47, Issue of November 22, pp. 44597–44605, 2002
Printed in U.S.A.

Substrate-dependent Competency of the Catalytic Triad of Prolyl Oligopeptidase*

Received for publication, July 23, 2002
Published, JBC Papers in Press, September 11, 2002, DOI 10.1074/jbc.M207386200

Zoltán Szeltner‡, Dean Rea§, Tünde Juhász‡, Veronika Renner‡, Zoltán Mucsi¶, György Orosz¶, Vilmos Fülöp§‖, and László Polgár‡**

From the ‡Institute of Enzymology, Biological Research Center, Hungarian Academy of Sciences, H-1518, P. O. Box 7, Budapest 112, Hungary, the §Department of Biological Sciences, University of Warwick, Gibbet Hill Road, Coventry CV4 7AL, United Kingdom, and ¶Department of Organic Chemistry, L. Eötvös University, Budapest H-1117, Pázmány Péter Sétány 1/A, Budapest 112, Hungary

Prolyl oligopeptidase, a serine peptidase unrelated to trypsin and subtilisin, is implicated in memory disorders and is an important target of drug design. The catalytic competence of the Asp^{641} residue of the catalytic triad (Ser^{554}, Asp^{641}, His^{680}) was studied using the D641N and D641A variants of the enzyme. Both variants displayed 3 orders of magnitude reduction in k_{cat}/K_m for benzyloxycarbonyl-Gly-Pro-2-naphthylamide. Using an octapeptide substrate, the decrease was 6 orders of magnitude, whereas with Z-Gly-Pro-4-nitrophenyl ester there was virtually no change in k_{cat}/K_m. This indicates that the contribution of Asp^{641} is very much dependent on the substrate-leaving group, which was not the case for the classic serine peptidase, trypsin. The rate constant for benzyloxycarbonyl-Gly-Pro-thiobenzylester conformed to this series as demonstrated by a method designed for monitoring the hydrolysis of thiolesters in the presence of thiol groups. Alkylation of His^{680} with Z-Gly-Pro-CH_2Cl was concluded with similar rate constants for wild-type and D641A variant. However, kinetic measurements with Z-Gly-Pro-OH, a product-like inhibitor, indicated that the His^{680} is not accessible in the enzyme variants. Crystal structure determination of these mutants revealed subtle perturbations related to the catalytic activity. Many of these observations show differences in the catalysis between trypsin and prolyl oligopeptidase.

The catalytic triad, which consists of serine, histidine, and aspartate residues, is an essential part of the catalytic machinery of serine peptidases. The role of Ser^{195} and His^{57} in chymotrypsin catalysis is firmly established, but the contribution of Asp^{102} to the catalysis has been the subject of a long discussion, following the discovery of a hydrogen bond between the catalytic His^{57} and Asp^{102}. It was postulated that the three residues form a charge-relay system, in which the proton of the Ser^{195} OH group was mediated by the His^{57} imidazole to the Asp^{102} carboxylate ion (1). This assumption was questioned on the basis of the chemical properties of the interacting groups, which render the proton transfer from the basic serine OH group to an acidic carboxyl group highly unlikely (2). The lack of proton transfer to the aspartate residue was confirmed by NMR (3–5) and neutron diffraction experiments (6). Further proposals have suggested that the catalytic triad serves as a charge stabilizing system, in which the aspartate ion stabilizes the protonated histidine. This species interacts with the negatively charged tetrahedral intermediate. It was also suggested that Asp^{102} may participate in the correct orientation of the tautomer of His^{57}, which is essential for accepting the proton from the Ser^{195} (2, 7–10).

The catalytic histidine (His^{57}) of the trypsin-type enzymes functions as a general base catalyst that assists the proton transfer from the serine OH to the leaving group of the substrate through the formation of a tetrahedral intermediate on the reaction path. This process generates an acyl enzyme, which is subsequently hydrolyzed by the reverse mechanism of acylation (10, 11). In the native trypsin, Nϵ2 of the catalytic histidine is the basic nitrogen atom that accepts the proton from the serine OH, whereas the protonated Nδ1 forms a hydrogen bond with the Asp^{102}. The catalytic triad of trypsin was investigated by substituting the neutral Asn for Asp^{102} (12, 13). It was concluded from the observed 4-orders of magnitude decrease in rate, as well as from x-ray crystallographic studies, that the modified enzyme held the unfavorable tautomer form of His^{57} that was unable to accept the proton from the serine OH group. Specifically, the Nϵ2 of His^{57} was protonated, and the basic Nδ1 formed a hydrogen bond with the NH_2 group of Asn^{102} (12). When both the Nδ1 and Nϵ2 atoms were protonated, His^{57} adopted an alternative conformation and interacted with a solvent water molecule rather than with the Asn^{102} residue.

Here we have examined the catalytic triad of prolyl oligopeptidase, which is a member of a relatively new group of serine peptidases, unrelated to the well known trypsin and subtilisin families. The new family includes enzymes of different specificities, like the prolyl oligopeptidase itself, dipeptidyl-peptidase IV, acylaminoacyl-peptidase, and oligopeptidase B (14–17). They share the way of selecting and cleaving substrates of no longer than about 30 amino acid residues in total. Prolyl oligopeptidase (EC 3.4.21.26) is implicated in the metabolism of peptide hormones and neuropeptides (18–20). Because specific inhibitors relieve scopolamine-induced amnesia (21–24), the enzyme is of pharmaceutical interest. The activity of prolyl oligopeptidase has also been associated with depression (25, 26) and blood pressure regulation (27).

* This work was supported by Wellcome Trust Grants 060923/Z/00/Z and 066099/01/Z, Human Frontier Science Program Grant RG0043/2000-M 102, Hungarian Science Foundation T/11 Grant T029056, and the British-Hungarian Science and Technology Program GB 18/98. The costs of publication of this article were defrayed in part by the payment of page charges. This article must therefore be hereby marked "*advertisement*" in accordance with 18 U.S.C. Section 1734 solely to indicate this fact.

The atomic coordinates and structure factors (code 1o6f and 1o6g) have been deposited in the Protein Data Bank, Research Collaboratory for Structural Bioinformatics, Rutgers University, New Brunswick, NJ (http://www.rcsb.org/).

‖ Royal Society University Research Fellow.

** To whom correspondence should be addressed. Tel.: 36-1-279-3110; Fax: 36-1-466-5465; E-mail: polgar@enzim.hu.

The three-dimensional structure determination of prolyl oligopeptidase has revealed that the carboxyl-terminal peptidase domain of the enzyme displays an α/β hydrolase fold and that its catalytic triad (Ser^{554}, His^{680}, Asp^{641}) is covered by the central tunnel of an unusual β-propeller (28). Recent engineering of the enzyme provided evidence for a novel strategy of regulation, in which oscillating propeller blades act as a gating filter during catalysis, letting small peptide substrates into the active site while excluding large proteins to prevent accidental proteolysis in the cytosol (29).

This work concentrates on two variants of prolyl oligopeptidase (D641N and D641A), which were prepared for studying the catalytic competence of Asp^{641}. It is anticipated that the alanine residue is not able to stabilize the catalytic histidine in the unfavorable tautomer form, as found with D102N trypsin. Hence, the study of the two variants may permit discrimination between the charge and the hydrogen-bonding effects of the Asp^{641} on the imidazole ring.

EXPERIMENTAL PROCEDURES

Enzyme Preparation—Prolyl oligopeptidase from porcine brain and its variants were expressed in *Escherichia coli* JM105 cells and purified as described previously (30). The enzyme concentrations were determined at 280 nm (16). Mutations were introduced with the two-step polymerase chain reaction as described for the Y473F mutant (30). The following primers were used to produce the D641N mutant: 5′-CTCACaGCtGACCACaAcGACCGA-3′ and 3′-GAGTGtCGaCTGGTGtTgCTGGCT-5′. An extra recognition site for *Pvu*II restriction enzyme (underlined) was also created with silent mutations. The primers for the D641A mutation were as follows: 5′-GCCGACCACGcgGACCGAGTGGTCC-3′ and 3′-CGGCTGGTGCgcCTGGCTCACCAGG-5′. An *Rsr*II restriction site (underlined) was also introduced with the alanine codon (GCG), which was used to verify the incorporation of the mutant oligonucleotides into the PCR product.

Kinetics—The reaction of prolyl oligopeptidase with Z-Gly-Pro-Nap (Bachem Ltd., Bubendorf, Switzerland) was measured fluorometrically, using a Cary Eclipse fluorescence spectrophotometer equipped with a Peltier four-position multicell holder accessory and a temperature controller. The excitation and emission wavelengths were 340 and 410 nm, respectively. Cells with excitation and emission path-lengths of 1.0 and 0.4 cm, respectively, were used. The substrate with internally quenched fluorescence, Abz-Gly-Phe-Gly-Pro-Phe-Gly-Phe(NO_2)-Ala-NH_2, was prepared with solid phase synthesis, and its hydrolysis was followed as in the case of Z-Gly-Pro-Nap, except that the excitation and emission wavelengths were 337 and 420 nm, respectively. The liberation of 4-nitrophenol from Z-Gly-Pro-ONp was monitored spectrophotometrically at 400 nm. The hydrolysis of Z-Gly-Pro-SBzl was measured at 240 nm, which indicated the decrease in the absorbance of the thiolester.

The pseudo-first order rate constants were measured at substrate concentrations lower than 0.1 K_m and were calculated by nonlinear regression data analysis, using the GraFit software (31). The specificity rate constants (k_{cat}/K_m) were obtained by dividing the first order rate constant by the total enzyme concentration in the reaction mixture.

The Michaelis-Menten parameters (k_{cat} and K_m) were determined with initial rate measurements, using substrate concentrations in the range of 0.2 to 5 K_m value. Because of the poor solubility of Z-Gly-Pro-Nap, in particular in the presence of 0.5 M NaCl, the reactions were carried out in the presence of 0.25% acetonitrile, which caused about 20% inhibition of prolyl oligopeptidase. The kinetic parameters were calculated with nonlinear regression analysis. At very low K_m the parameters were calculated from progress curves using the integrated Michaelis-Menten equation (32, 33).

Theoretical curves for the bell-shaped pH-rate profiles were calculated by nonlinear regression analysis, using Equation 1 (below) and the GraFit software (31). In Equation 1, k_{cat}/K_m(limit) stands for the pH-independent maximum rate constant, and K_1 and K_2 are the dissociation constants of catalytically competent base and acid, respectively. When an additional ionizing group modifies the bell-shaped character of the pH dependence curve, the data were fitted to Equation 2 (doubly bell-shaped) or Equation 3 (doubly bell-shaped curve with double ionization at the basic limb) (below). The limiting values in the equations stand for the pH-independent maximum rate constants for the two active forms of the enzyme, and K_1, K_2, K_3, and K_x are the apparent dissociation constants of the enzymatic groups, whose state of ionization controls the rate constants.

$$k_{cat}/K_m = k_{cat}/K_m(\text{limit})[1/(1 + 10^{pK_1-pH} + 10^{pH-pK_2})] \quad \text{(Eq. 1)}$$

$$k_{cat}/K_m = k_{cat}/K_m(\text{limit})_1[1/(1 + 10^{pK_1-pH} + 10^{pH-pK_2})] + k_{cat}/K_m(\text{limit})_2[1/(1 + 10^{pK_2-pH} + 10^{pH-pK_3})] \quad \text{(Eq. 2)}$$

$$k_{cat}/K_m = k_{cat}/K_m(\text{limit})_1[1/(1 + 10^{pK_1-pH} + 10^{pH-pK_2})] + k_{cat}/K_m(\text{limit})_2[1/(1 + 10^{pK_2-pH} + 10^{pH-pK_3} + 10^{2pH-pK_3-pK_x})] \quad \text{(Eq. 3)}$$

Determination of Dissociation Constants—The K_i values, the dissociation constants of the enzyme·inhibitor complex, were calculated from Equation 4, below, where k_i and k_0 are pseudo-first order rate constants determined at substrate concentrations $< 0.1\ K_m$ in the presence and absence of inhibitor (I), respectively. In the case of slow reactions initial rates were measured instead of the first order rate constants.

$$k_i/k_0 = 1/(1 + I/K_i) \quad \text{(Eq. 4)}$$

The dissociation constant for an internally quenched substrate was determined by measuring the fluorescence change upon binding of the substrate to the inactive S554A variant of prolyl oligopeptidase. The formation of enzyme·substrate complex at similar concentrations of the enzyme and substrate is described by Equation 5, shown below, when the conditions for the Michaelis-Menten equation do not meet (34), and by Equation 6, where ES and K_s are the enzyme-substrate complex and its dissociation constant, respectively.

$$E\text{S} = ((S_0 + E + K_s) - \text{sqrt}(\text{sqr}(S_0 + E + K_s) - 4E^*S_0))/2 \quad \text{(Eq. 5)}$$

$$\Delta F = \Delta F_{max}{}^*((S_0 + E + K_s) - \text{sqrt}(\text{sqr}(S_0 + E + K_s) - 4E^*S_0))/2^*S_0 \quad \text{(Eq. 6)}$$

The substrate (S_0) was saturated with increasing amounts of enzyme (E). Although ES is not known, its concentration is proportional to the change in the fluorescence signal, measured at 328- and 420-nm excitation and emission wavelengths, respectively. Hence, Equation 5 can be transformed into Equation 6, where ΔF corresponds to ES, and ΔF_{max} gives the change in signal when the substrate is completely converted into the enzyme·substrate complex. A plot of ΔF against E gives K_s and ΔF_{max} using nonlinear regression.

Alkylation with Peptidyl-chloromethane—The Z-Gly-Pro-CH_2Cl was prepared from Z-Gly-Pro-OH (Bachem Ltd.) by preparing the diazomethyl intermediate (21, 35), which was then transformed into the product as described previously (36). The oily compound was purified by chromatography. The inactivation of prolyl oligopeptidase by the irreversible inhibitor, Z-Gly-Pro-CH_2Cl, was followed in the presence of substrate (37, 38) under pseudo-first order conditions ($I_0 \gg E_0$). Z-Gly-Pro-Nap or suc-Gly-Pro-Nan was used as substrates at high enough concentrations so that less than 10% of substrate was consumed during the complete inactivation of the enzyme. The first order apparent rate constant of inactivation, k_{app}, was calculated from Equation 7, shown below, where P and P_{inf} are the concentrations of the product at times t and t infinite (when the enzyme is completely inactivated), respectively. If k_{app}, which is dependent on the inhibitor concentration, is plotted against I, k_{inact} and K_i(app) can be obtained from Equation 8, shown below, using nonlinear regression analysis. Under the conditions employed $S_0 \ll K_m$, therefore $K_i(\text{app}) = K_i$.

$$P = P_{inf}(1 - \exp(-k_{app}t)) + \text{offset} \quad \text{(Eq. 7)}$$

$$k_{app} = k_{inact}I_0/(I_0 + K_{i(app)}) \quad \text{(Eq. 8)}$$

Crystallization, X-ray Data Collection, and Structure Refinement—Both D641A and D641N mutants were co-crystallized in the presence of substrate suc-Gly-Pro-Nan using the conditions established for the wild-type enzyme (28). Crystals belong to the orthorhombic space group $P2_12_12_1$ with cell dimensions a = 71.4 Å, b = 100.2 Å, c = 111.3 Å for the D641A, and a = 71.6 Å, b = 100.6 Å, c = 111.1 Å for the D641N mutant. X-ray diffraction data were collected at 100 K on an ADSC Q4 CCD detector. Data were processed using the HKL suite of programs (39). Refinements of the structures were carried out by alternate cycles of X-PLOR (40) and manual refitting using O (41), based on the 1.4-Å resolution model of wild-type enzyme (14) (PDB code 1qfm). A bulk solvent correction allowed all measured data to be used. Water mole-

TABLE I
Data collection and refinement statistics

	D641A	D641N
Data collection		
Synchrotron radiation	ESRF ID14–1	SRS 9.6
Synchrotron wavelength (Å)	0.934	0.87
Resolution (Å)	52–1.6	30–1.4
Observations	683,945	686,744
Unique reflections	103,351	156,733
R_{sym} [a]	0.136	0.053
Completeness (%)	97.7	99.1
Refinement		
Non-hydrogen atoms	6,461 (including 3 glycerol and 726 water molecules)	6,796 (including 1,074 water molecules)
R_{cryst} (2σ) [b]	0.202	0.200
Reflections used	97,466	149,158
R_{free} (2σ) [c]	0.221	0.216
Reflections used	4,137	6,284
R_{cryst} [b]	0.208	0.202
Reflections used	99,145	150,408
R_{free} [c]	0.228	0.217
Reflections used	4,206	6,325
R_{cryst} (all data) [b]	0.209	0.203
Mean temperature factor (Å^2)	13.1	15.1
r.m.s. deviations from ideal values		
Bonds (Å)	0.008	0.008
Angles (°)	1.5	1.4
Mean coordinate error (Å) [d]	0.07	0.08

[a] $R_{sym} = \Sigma_j\Sigma_h|I_{h,j} - \langle I_h\rangle|/\Sigma_j\Sigma_h\langle I_h\rangle$, where $I_{h,j}$ is the jth observation of reflection h, and $\langle I_h\rangle$ is the mean intensity of that reflection.
[b] $R_{cryst} = \Sigma||F_{obs}| - |F_{calc}||/\Sigma|F_{obs}|$; where F_{obs} and F_{calc} are the observed and calculated structure factor amplitudes, respectively.
[c] R_{free} is equivalent to R_{cryst} for a 4% subset of reflections not used in the refinement (53).
[d] Determined by the SIGMAA method (50).

cules were added to the atomic model at the positions of large positive peaks (>3.0 σ) in the difference electron density, only at places when the resulting water molecule fell into an appropriate hydrogen-bonding environment. Restrained isotropic temperature factor refinements were carried out for each individual atom. The final model contains all the 710 amino acid residues in both complexes, the bound peptides, and a large number of solvent (glycerol and water) molecules. Statistics for the data processing and refinement are given in Table I.

RESULTS

pH-rate Profiles—The reaction of wild-type prolyl oligopeptidase with the Z-Gly-Pro-Nap substrate has revealed two pH-dependent enzyme forms, arising from the change in the ionization state of some enzymatic group (30). The two forms prevail in the presence of 0.5 M NaCl, but the high salt concentration increases k_{cat}/K_m by a factor of about 2.5 (Table II). The pH rate profile of the D641N variant also displays doubly bell character both in the presence and the absence of 0.5 M salt (Fig. 1*A*). However, the points do not properly fit to the theoretical doubly bell curve (see Equation 2 and Fig. 1*A*, *thin line*), indicating that additional ionizing groups affect the reaction. Clearly, the sharper slopes, which involve the participation of two acidic groups in the alkaline pH range, better follow the experimental points (see Fig. 1*A*, *thick lines* and Equation 3). This decline in activity may be caused by reversible unfolding of the protein (42). Importantly, the rate constants are lower by 3 orders of magnitude than those obtained with the wild-type enzyme (Table II), and this underlines the essential role of the aspartate ion in the catalysis.

The activity of the D641A enzyme variant is also reduced by 3 orders of magnitude, although the rate constant is slightly higher than that for the D641N variant (Table II). In the absence of 0.5 M NaCl, the reaction of the D641A variant exhibits a virtually proper doubly bell-shaped pH-rate profile (Equation 2); namely, the additional acidic group observed with the D641N enzyme is not noticeable with the D641A variant (see Table II and Fig. 1*B*). In contrast to the D641N enzyme, the D641A variant gives a simple bell-shaped curve in the presence of salt. For the D641A variant, particularly at high salt concentration, the pH optimum is shifted toward the lower pH, so the activity of the low-pH form of the enzyme becomes predominant relative to the high-pH form.

The enhancement of rate with the increase in ionic strength is another difference between the wild-type enzyme and its variants. Compared with the wild-type enzyme, the rate increase is significantly less with the high-pH form of the D641N variant and practically does not change with the low pH form. In the case of the D641A variant, the effect of salt leads to an alteration in the pH-rate profile by eliminating the doubly bell character of the curve.

The pH dependences of the prolyl oligopeptidase variants are substantially different from that observed with the D102N trypsin. At neutral pH, the mutant trypsin was $\sim 10^4$ times less active than the unmodified enzyme. With the increase in pH, the activity increased considerably and approached that of the native enzyme. For these effects, a conclusive explanation could not be offered. The enhanced activity was assigned to the participation of either a titratable base or of a hydroxide ion (13). In the catalysis of the prolyl oligopeptidase variants, such a contribution has not been observed; the reduced activity was maintained over the entire pH range.

The Leaving Group Effect—The wild-type prolyl oligopeptidase exhibits similar activities toward the Z-Gly-Pro-Nap and an octapeptide substrate (Table III). As shown above, the rate constants for the reaction of the modified enzymes with Z-Gly-Pro-Nap diminish by 3 orders of magnitude (Table II). Unexpectedly, the D641A and D641N variants were 6 orders of magnitude less active (rate constants are 4.62 and 3.73 $M^{-1}s^{-1}$, respectively) than that of the native enzyme toward the octapeptide (Table III). Crystallographic studies revealed that the binding of the octapeptide is unaffected by the Asp^{641} mutation (data are not shown). The dramatic difference in activity implies that the contribution of the histidine residue is negligible to the catalysis of both enzyme variants. A similarly large decrease, *i.e.* 6 orders of magnitude, was found in the reaction of subtilisin with suc-Ala-Ala-Pro-Phe-Nan, when the catalytic histidine was eliminated by replacement with an alanine (43).

TABLE II
Kinetic parameters for the reactions of prolyl oligopeptidase variants with Z-Gly-Pro-Nap

	$k(\text{limit})_1$	$k(\text{limit})_2$	pK_1	pK_2	pK_3	pK_x
	$mM^{-1}\ s^{-1}$					
Wild-type[a]	1750 ± 200	5070 ± 220	4.88 ± 0.31	7.47 ± 0.13	9.16 ± 0.06	
+0.5 M NaCl[a]	5090 ± 240	12,820 ± 690	5.20 ± 0.10	7.74 ± 0.11	8.73 ± 0.06	
D641 N	1.51 ± 0.08	3.83 ± 0.77	5.96 ± 0.09	9.02 ± 0.27	10.16 ± 0.32	8.02 ± 0.34
+0.5 M NaCl	1.66 ± 0.23	5.44 ± 1.05	6.29 ± 0.19	8.63 ± 0.27	10.23 ± 0.35	7.59 ± 0.35
D641A	4.02 ± 0.56	13.09 ± 0.96	5.84 ± 0.15	7.80 ± 0.15	8.88 ± 0.07	
+0.5 M NaCl		10.65 ± 0.29[b]	6.59 ± 0.04		8.74 ± 0.05	

[a] From Ref. 48.
[b] $k(\text{limit})$ of Equation 1 rather than $k(\text{limit})_2$.

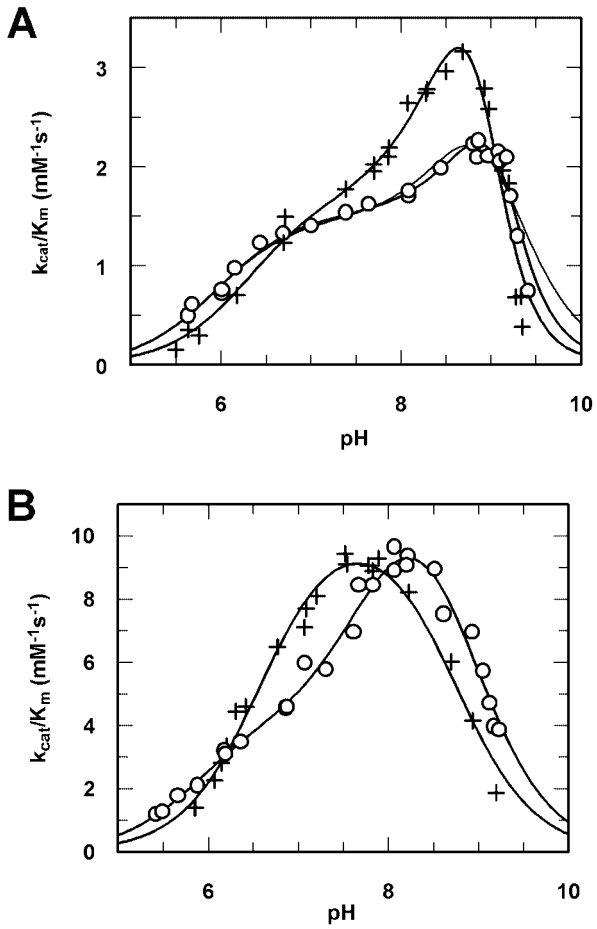

FIG. 1. **The pH dependences of the reactions of prolyl oligopeptidase variants.** The data were measured in the absence (○) and presence (+) of 0.5 M NaCl. *A*, D641N variant; the *thick lines* are calculated with Equation 3. The *thin line* is a doubly bell-shaped curve derived from Equation 2. *B*, D641A variant. The *points* conform to a bell-shaped and a doubly bell-shaped curve in the presence and in the absence of 0.5 M NaCl, respectively.

As for the D641N and D641A enzyme variants, the different rates of hydrolysis of the octapeptide and the naphthylamide substrates may arise from the greater strength of the peptide bond compared with the strength of the scissile bond of the naphthylamide substrate. Apparently, the defective active site is less effective against the stronger bond. As mentioned above, it is the catalysis, not the binding, that is impaired. Indeed, the K_m values are similar for the reactions of the wild-type enzyme and its variants when tested with Z-Gly-Pro-Nap (Table III). The K_m values were shown to approach K_s, the enzyme-substrate dissociation constant with peptide and amide substrates in the case of serine peptidases (10, 11). The binding of the octapeptide, not perturbed by a subsequent catalytic step, was measured by using an inactive variant (S554A) of prolyl oligopeptidase, as described under "Experimental Procedures." The determination exploited the internal quenching of the octapeptide, which was abolished upon binding to the peptidase (Fig. 2). The results have shown that the binding constant, K_s, does not change too much upon modification of the aspartate of the catalytic triad (Table III). Interestingly, the binding seems to be stronger with the enzyme variant. The K_m and K_s for the octapeptide could not be compared, because the former was measured with the native enzyme, and the latter was measured with the inactive S554A variant.

The above results suggest that the hydrolysis of a substrate possessing a better leaving group deteriorates to a lesser extent as a result of the modification of Asp^{641}. Therefore, we have examined the hydrolysis of Z-Gly-Pro-ONp, which has a very good leaving group, 4-nitrophenol. The reactions were carried out at pH 7.0, where the spontaneous hydrolysis of the substrate was less significant than at higher pH. The rate constants were corrected for the non-enzymatic hydrolysis, still present at pH 7. Interestingly, the specificity rate constants for the enzyme variants did not change appreciably, whereas k_{cat} and K_m both diminished by 3 orders of magnitude (Table III).

In the reaction of the wild-type enzyme with Z-Gly-Pro-ONp, the formation of the acyl enzyme (k_{cat}/K_m) is the rate-determining step (44), and this appears to change to deacylation (k_3) with the modified enzymes. The rate constants are defined by Equations 9 and 10, below, where *E*S is the enzyme·substrate complex, *E*A refers to the acyl enzyme, and P_1 and P_2 are the reaction products. The k_{cat}/K_m is a complex constant that involves not only the dissociation constant of the enzyme substrate complex ($K_s = k_{-1}/k_1$) and k_2 but also a substrate-induced conformational change (45).

$$E + S \underset{k_{-1}}{\overset{k_1}{\rightleftharpoons}} ES \overset{k_2}{\searrow} EA \overset{k_3}{\searrow} E \qquad \text{(Eq. 9)}$$
$$\qquad\qquad\qquad\quad P_1 \qquad\quad P_2$$

$$E + S \xrightarrow{k_{cat}/K_m} EA + P_1 \qquad \text{(Eq. 10)}$$

The decrease of a similar magnitude in both k_{cat} and K_m can be interpreted in several ways. (i) The binding and the rate constant change to the same extent. However, this is not supported by the small change in the K_s values for the octapeptide, as shown in Table III. Otherwise, it is highly unlikely that the binding would decrease by 3 orders of magnitude while the main features of the binding site (S4-S2′) remain intact. (ii) Compensatory changes in k_{cat} and K_m are known to refer to nonproductive binding (8). Again, it is doubtful that the nonproductive binding would emerge in the variant but not in the wild-type enzyme. (iii) A reasonable explanation may be that the decrease in K_m arises from a change in the rate-determining step, so that acylation is rate-determining with the wild-type enzyme, and deacylation is rate-determining with its variants. This is conceivable, because general base catalysis is not required in acylation when the substrate has a good leaving

TABLE III
Kinetic parameters for prolyl oligopeptidase and its variants in the presence of 0.5 M NaCl concentration

	Wild-type	D641N	D641A
Z-Gly-Pro-Nap[a]			
k_{cat} (s^{-1})	32.5 ± 1.2	0.0151 ± 0.0007	0.0657 ± 0.0031
K_m (μM)	5.9 ± 0.5	13.5 ± 1.1	5.4 ± 0.6
k_{cat}/K_m (μM^{-1} s^{-1})	5.507	0.00116	0.012
Octapeptide[b]			
k_{cat} (s^{-1})	5.38 ± 0.24[c]		
K_m (μM)	2.05 ± 0.34[c]		
k_{cat}/K_m	2.62 ($\mu M^{-1} s^{-1}$)[c]	3.73 ± 0.07 (M^{-1} s^{-1})[d]	4.62 ± 0.13 (M^{-1} s^{-1})[d]
K_s (μM)[e]	23.8 ± 0.9		5.8 ± 1.4
Z-Gly-Pro-ONp[f]			
k_{cat} (s^{-1})	36 ± 2.4	0.021 ± 0.001	0.031 ± 0.001
K_m (μM)	19.2 ± 3.7	0.028 ± 0.003	0.025 ± 0.004
k_{cat}/K_m (μM^{-1} s^{-1})	1.87 (4.72)	0.75	1.24
Z-Gly-Pro-SBzl[g]			
k_{cat} (s^{-1})	108 ± 16	0.028 ± 0.014	0.099 ± 0.027
K_m (μM)	16.0 ± 2.1	1.52 ± 0.71	1.59 ± 0.52
k_{cat}/K_m (μM^{-1} s^{-1})	6.76	0.018	0.062

[a] pH 7.0, 0.25% acetonitrile.
[b] Abz-Gly-Phe-Gly-Pro-Phe-Gly-Phe(NO_2)-Ala-NH_2.
[c] pH 8.0, no NaCl was added (30).
[d] Measured under pseudo-first order conditions, pH 8.0, at 0.31 μM substrate concentration, without salt.
[e] pH 8.0, no NaCl was added. The binding of the octapeptide was determined with the inactive C554A enzyme variant.
[f] pH 7.0, 0.3% acetonitrile.
[g] pH 7.0, 0.1% acetonitrile.

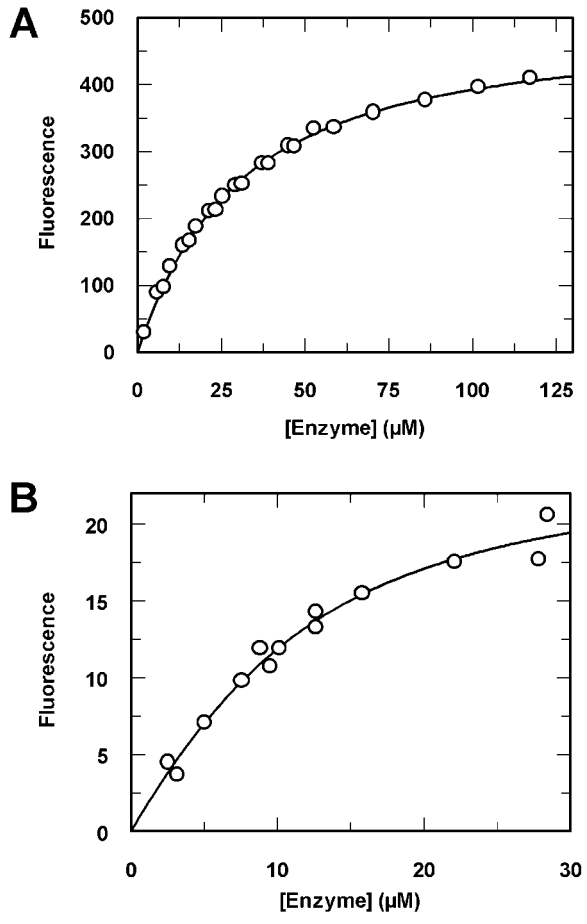

FIG. 2. **Determination of the dissociation constants for the prolyl oligopeptidase·Abz-Gly-Phe-Gly-Pro-Phe-Gly-Phe(NO_2)-Ala-NH_2 complexes.** The peptide (9.3 μM) was titrated with increasing amounts of S554A enzyme variant *A* and S554A/D641A variant *B* at pH 8.0. The theoretical curves were calculated by using Equation 6. The *points* in *Panel A* are from two independent experiments.

group. However, general base catalysis is essential for deacylation. Accordingly, the ratio of k_3/k_2 changes with the enzyme variants and modifies $K_m = K_s k_3/(k_2+k_3)$. Hence, if $k_2 \gg k_3$, as in the enzyme variants, then $K_m = K_s(k_3/k_2)$, and thus $K_m \ll K_s$. Of course, $k_{cat} = k_2k_3/(k_2+k_3)$ decreases to the same extent, because the rate-limiting step from k_2 for the wild-type enzyme changes to $k_{cat} = k_2(k_3/k_2) = k_3$ for the variants. With the naphthylamide substrate lacking a good leaving group, the K_m values for the wild-type enzyme and its variants are not very different, as the rate-determining step (k_2) does not change.

In addition to the nitrophenyl ester, we have investigated the thiolester, Z-Gly-Pro-SBzl, because the thioalcohol is also a good leaving group although not as good as the 4-nitrophenol. The study of the thiolester is required if the present results are to be compared with those obtained from the kinetic studies on D102N trypsin, because the latter study was performed with a thiolester substrate (13). The hydrolysis of thiobenzyl esters is generally measured in the presence of 5,5′-dithiobis(2-nitrobenzoate) or 4,4′-dipyridyl disulfide (46). This method was not applicable to prolyl oligopeptidase, which has a number of thiol groups. Moreover, the reaction mixture contains dithioerythritol. Therefore, we exploited the UV absorbance of the thiolester, possessing a maximum of about 240 nm, which diminished during the hydrolysis. It was found that the thiolester exhibited an intermediary behavior between the nitrophenyl ester and the naphthylamide substrates (Table III). The 3-orders of magnitude decrease in k_{cat} was only partly compensated by the 1-order of magnitude decrease in K_m. This indicated that the inhibitory effect manifested in k_2 for Z-Gly-Pro-SBzl is intermediate between the k_2 values for Z-Gly-Pro-Nap and Z-Gly-Pro-ONp.

Inhibitor Binding—We have shown recently that Z-Gly-Pro-OH is a product-like competitive inhibitor of prolyl oligopeptidase (47). The association constant ($1/K_i$) for the enzyme·inhibitor complex increased with the decrease in pH, as the catalytic His^{680} became protonated and formed a strong salt bridge with the carboxylate ion of the inhibitor. This made it possible to titrate the true pK_a of the catalytic histidine of the wild-type enzyme, which resulted in a value of 6.2 both with and without 0.5 M NaCl.

In the absence of 0.5 M NaCl, a simple K_i could not be obtained for the complex of Z-Gly-Pro-OH with either the D641N or the D641A enzyme variant. Namely, the experimental points departed from the curve defined by Equation 4 (Fig. 3*A*), and the data conformed to a doubly exponential decay, suggesting that

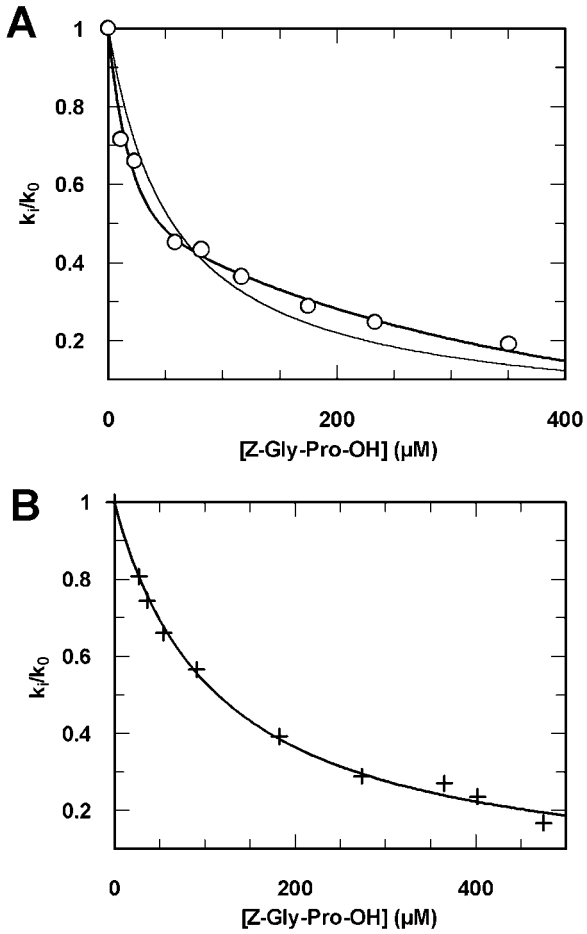

FIG. 3. **Inhibition of prolyl oligopeptidase D641A variant with Z-Gly-Pro-OH.** *A*, first order rate constants were measured with 2–3 μM enzyme at pH 6.45 without added salt. The *points* were fitted to Equation 4 (*thin line*) or to a double exponential decay (*thick line*). *B*, in the presence of 0.5 M NaCl the data adhere to Equation 4 even at the slightly alkaline pH of 7.45.

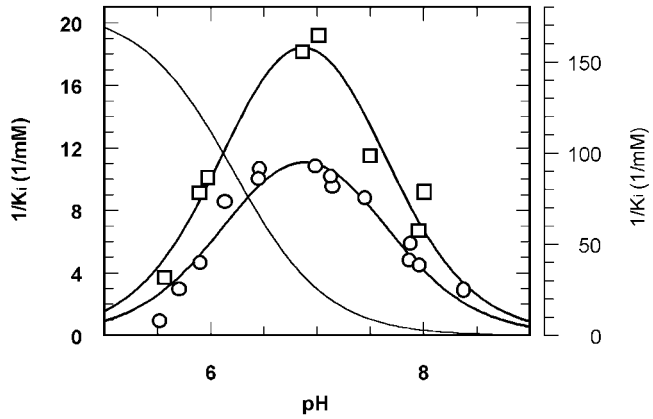

FIG. 4. **Complex formation between Z-Gly-Pro-OH and the D641A variant of prolyl oligopeptidase.** The K_i values were determined in the presence of 0.5 M NaCl using Equation 4. The *thin line* and the *second y-axis scale* refer to the wild-type enzyme (47). The *circle* and *square* represent the D641A and D641N variants. The parameters for the curves are shown in Table IV. The first order rate constants for the enzyme variants (0.25–1.0 μM) were measured with Z-Gly-Pro-Nap.

TABLE IV
pH dependence of the association constant for Z-Gly-Pro-OH with prolyl oligopeptidase and its variant

	Wild-type[a]	D641A	D641N
$1/K_i$(limit)	226 ± 7	15.7 ± 1.8	26.2 ± 3.6
pK_1	6.22 ± 0.05	6.21 ± 0.11	6.20 ± 0.13
pK_2		7.56 ± 0.12	7.54 ± 0.15

[a] From Ref. 47.

TABLE V
Inhibition and inactivation constants for the reactions with Z-Gly-Pro-CH_2Cl measured in the presence of 0.5 M NaCl at pH 7.0

	C225A (A)	C225A/D641A (B)	B/A
K_i (nM)[a]	24 ± 2	87 ± 2	3.6
k_{inact} (h^{-1})[b]	1.08 ± 0.05	0.34 ± 0.01	0.3

[a] Determined with the method using Equation 4.
[b] From the progress curve method, using Equation 7, at saturation concentration of inhibitor when $k_{app} = k_{inact}$. The inhibitor concentrations were 800 and 1700 nM for the C255A and C255A/D641A enzyme variants, respectively.

the inhibitor binding was of a complex type. In the absence of salt, appropriate fitting was observed only below pH 6.

Using the D641A variant, we obtained correct fitting at 0.5 M NaCl concentration (Fig. 3*B*). Therefore, the pH dependence of $1/K_i$ was determined in the presence of 0.5 M NaCl. The association constants were plotted against pH. The acidic limb of the resulting bell-shaped curve did not fit properly to the points and suggested that at least two ionizing groups accounted for the deviation (Fig. 4). In the low pH range, where $1/K_i$ for the wild-type enzyme increased (*thin line* in Fig. 4), the association constant for the enzyme variant decreased rather than increased and provided substantially lower values for $1/K_i$. This may account for the considerably reduced association constant, in particular at low pH. A similar pH dependence was obtained with the D641N variant at 0.5 M NaCl concentration, indicating that the catalytic histidine of this enzyme variant cannot be titrated either. However, the association constant of the inhibitor was somewhat higher than that of the D641A variant (Table IV). At low pH, when double protonated, the imidazole group of His^{680} may change conformation, and thus it cannot form a salt bridge with the carboxyl group of the inhibitor. However, this would require an unfavorable conformation of His^{680} (see below). As for the wild-type enzyme, the acidic form of the imidazole group with a pK_a of 6.2 is responsible for binding (47). In contrast, with the modified enzyme a basic group with a pK_a of 6.2 is the competent form in the acidic pH range, as is an acid with a pK_a of 7.5 above neutrality. The weakening of binding in the acidic region is not consistent with an ionic interaction between the protonated histidine and the inhibitor, indicating that the protonated imidazole is not available for the carboxylate group of the inhibitor.

Alkylation of the Catalytic Histidine—In the case of the D102N trypsin variant the rate of alkylation of the active site histidine lowered by about a factor of 3–5 (13), which is a slight effect compared with the damage in the catalysis. Using Z-Gly-Pro-CH_2Cl, we have alkylated prolyl oligopeptidase and its variant with similar results. For the alkylation studies, the C255A variant of prolyl oligopeptidase was used, because Cys^{255}, which is located at the binding site region, is a potential target of the alkylating agent (48), and its modification could interfere with the alkylation of histidine. The inactivation of the enzyme was followed in the presence of substrate under pseudo-first order conditions. The suc-Gly-Pro-Nan and Z-Gly-Pro-Nap were used in the reactions with the native and the modified enzymes, respectively, and k_{app} was calculated from Equation 7. Because K_i, the dissociation constant of the enzyme·inhibitor complex was low, the condition that I_0 must be much higher than E_0 could not be satisfied appropriately. Therefore, k_{app} was determined at high concentrations of inhibitor (>50 K_i), where it was equal to k_{inact}. The inactivation

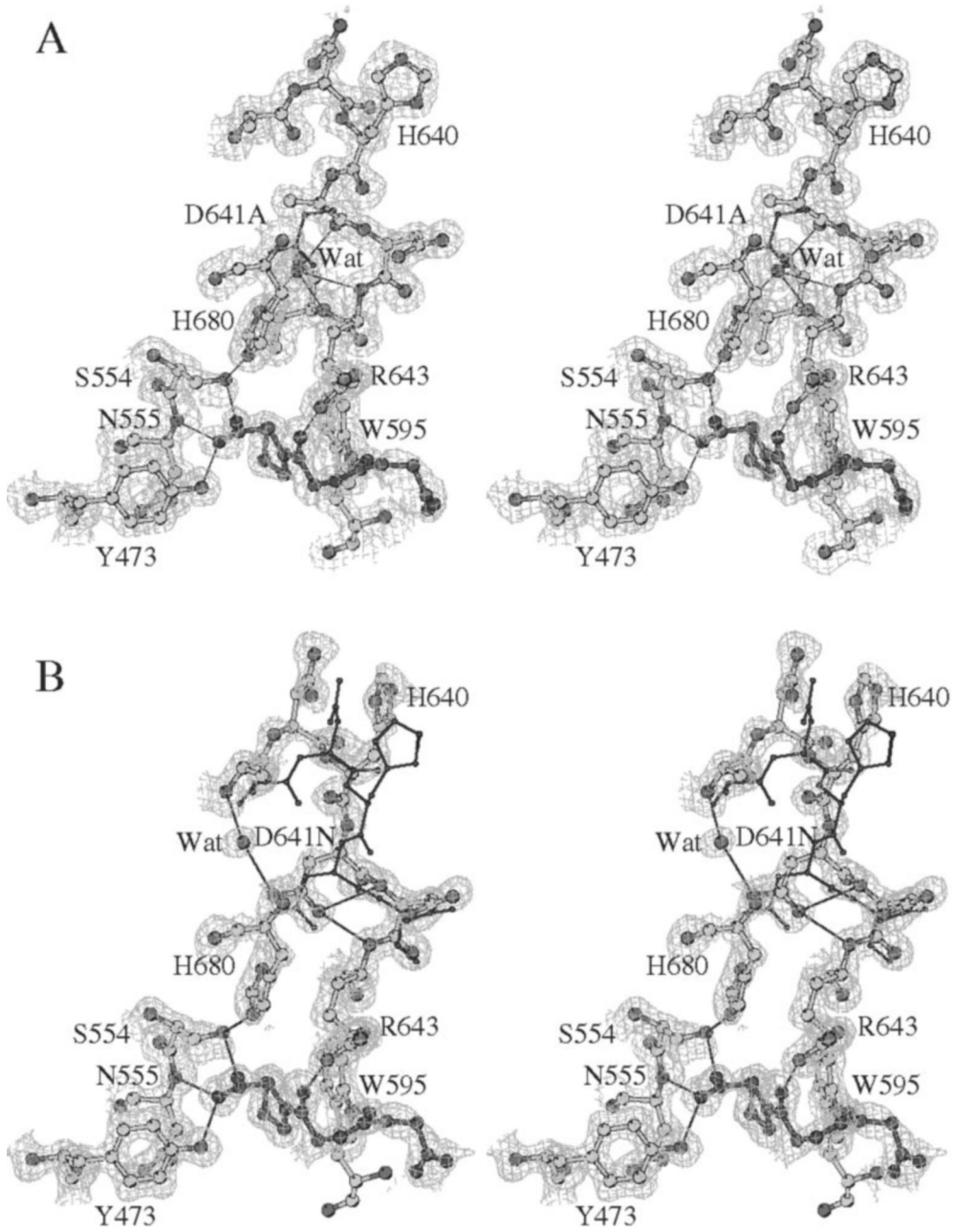

FIG. 5. **Stereo view of the mutated site of prolyl oligopeptidase.** *A*, D641A variant; the corresponding Asp^{641} side chain is shown as the *thin line*. *B*, D641N variant. Residues 638–643 of the wild-type enzyme are shown as *thin lines* (from PDB entry 1qfm). The hydrolyzed substrate suc-Gly-Pro-OH is shown darker than the protein residues. The SIGMAA (50) weighted $2mF_o - \Delta F_c$ electron density using phases from the final model is contoured at 1σ level, where σ represents the r.m.s. electron density for the unit cell. Contours more than 1.4 Å from any of the displayed atoms have been removed for clarity. *Dashed lines* indicate hydrogen bonds (drawn with MolScript; see Refs. 51 and 52).

was rather slow (Table V); the reduction in the rate constant for the C255A/D641A variant, relative to that for the C255A variant, was similarly small as found with trypsin and its D102N variant (13). This small change in alkylation compared with that observed in the substrate hydrolysis is conceivable considering the different characters of the two reactions. The transition state of the catalysis requires stabilization by the charged aspartate residue, but the simple alkylation does not. It was shown earlier that the reaction of prolyl oligopeptidase with a peptidyl-chloromethane resulted in the formation of a covalent bond between the inhibitor and His^{680} (49).

Table V also shows the dissociation constant of the enzyme·inhibitor complex, K_i, calculated in an independent way. On the addition of Z-Gly-Pro-CH_2Cl, a reversible enzyme inhibitor complex formed immediately and remained practically stable, because the subsequent rate of alkylation was rather slow. This rendered it possible to determine the K_i, as in the case of Z-Gly-Pro-OH, using Equation 4.

Crystal Structures of the D641A and D641N Mutants—Fig. 5*A* illustrates the structural changes introduced by the D641A mutation. A water molecule occupies the position of the mutated carboxylate group hydrogen bonded to the Nδ1 atom of His^{680} (2.86 Å). This water molecule is also involved in further hydrogen bonds with the main-chain amide and carbonyl of Val^{644} (2.79 and 2.87 Å, respectively). The carbonyl of Ala^{641} and the amide of Arg^{643} are also within the upper limit of hydrogen bonding distance (3.1 Å), but a water molecule cannot have more than four contacts. The mutation and the presence

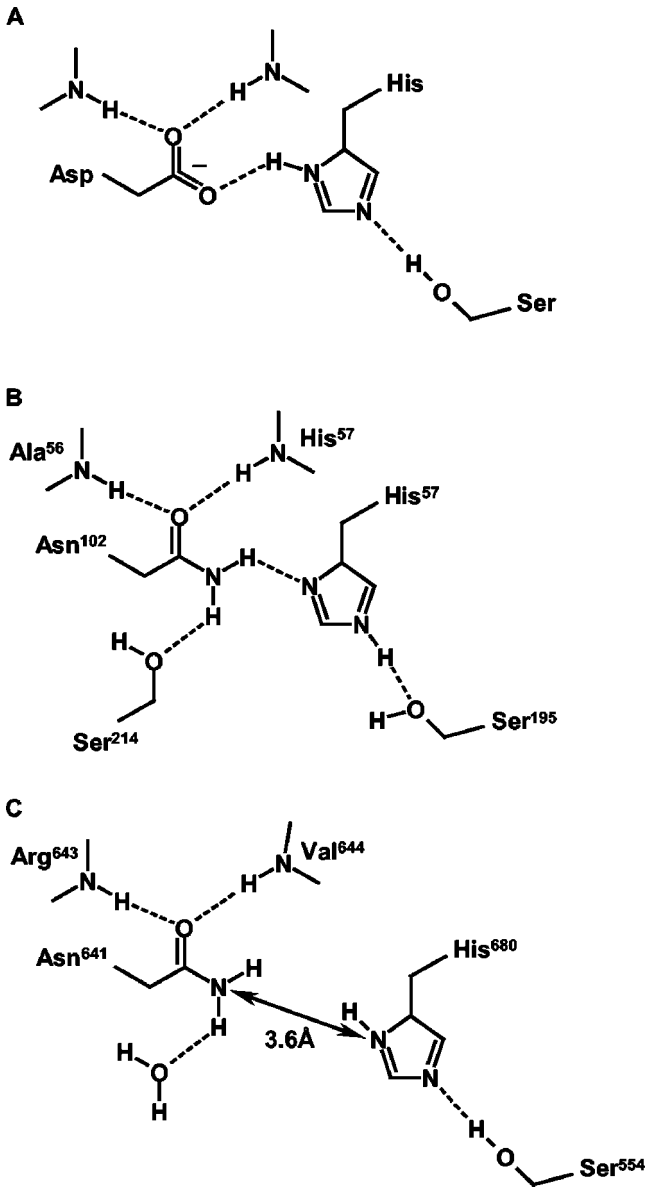

FIG. 6. **The catalytic triad and surrounding residues (*A*) standard catalytic triad (Asp, His, and Ser), (*B*) D102N trypsin (drawn from Ref. 12), and (*C*) D641N prolyl oligopeptidase.** Hydrogen bonds are shown as *dotted lines*. Distances are shown using *double-headed arrows*. The figure was drawn using ISIS Draw (www.mdli.com).

of this water molecule do not induce any further significant structural changes. The superposition of the structure with the wild-type enzyme gives a root mean square (r.m.s.)[1] deviation of 0.16 Å for all the Cα atoms and 0.24 Å for residues 638–643 in this region. However, more perturbation is observed in the D641N variant (Fig. 5*B*). Asn^{641} moves away from His^{680} pushing the loop containing residues 638–643 toward the surface of the molecule. The Oδ1 atom of Asn^{641} is hydrogen-bonded to main-chain amides of Asp^{642} and Arg^{643}, as was observed with the corresponding atom in the wild-type structure. The r.m.s. deviation of the Cα atoms in this region is 0.78 Å (0.36 Å including all Cα atoms) with the wild-type enzyme. The distance between Nδ2 of Asn^{641} and Nδ1 of His^{680} is too large (3.6 Å) to allow formation of a hydrogen bond. Both D641A and D641N mutants were crystallized in the presence of substrate suc-Gly-Pro-Nan; therefore the hydrolyzed product is bound to the active site in the usual manner (see Fig. 5; Protein Data Bank codes 1o6f and 1o6g) (47).

DISCUSSION

The role of the catalytic aspartate has been studied thoroughly in the reactions of trypsin and its D102N variant with suc-Ala-Ala-Pro-Arg-SBzl (12, 13). It was concluded that the nucleophilicity of the active site serine of the enzyme variant decreased as a result of the stabilization of the wrong tautomer of His^{57} that was unable to accept the serine hydroxyl proton. To exclude the stabilization of the incorrect tautomer of His^{680} of prolyl oligopeptidase, we have studied the D641A variant, in addition to the D641N variant. The similar reductions found in the k_{cat}/K_m values for these two enzyme variants suggested that the rate decrease could not be ascribed to the stabilization of an incompetent histidine tautomer. This finding is not peculiar to prolyl oligopeptidase, because the D32A variant of subtilisin experienced a similar decrease in activity, as did the trypsin D102N variant (43).

The pH-k_{cat}/K_m profiles for the prolyl oligopeptidase variants D641N and D641A maintain the doubly bell-shaped character of the wild-type enzyme. The pK_a values extracted from the curves are meaningless apparent parameters. The true pK_a of His^{680} could be titrated in the wild-type enzyme but not in the defective variants (Fig. 4). An interesting difference between the corresponding variants of trypsin and prolyl oligopeptidase was found in the alkaline pH region. With the trypsin variant the hydrolysis augmented substantially with the increase in pH (13), whereas with the prolyl oligopeptidase variants the pH-rate profiles essentially persisted, even at high pH. The reason for the distinct behavior is not clear.

As for the D102N variant of trypsin, it was claimed that the activity of the mutant enzyme toward a variety of substrates (12), specifically toward a thiolester and a nitroanilide (13), was reduced equally by 4 orders of magnitude. In contrast, with the prolyl oligopeptidase variant the k_{cat}/K_m was highly dependent upon the substrate employed. The change was virtually zero for the nitrophenyl ester and 6 orders of magnitude for the octapeptide substrate. This huge difference implies that the contribution of the catalytic triad is more needed when a stronger bond is to be cleaved.

The binding of the octapeptide substrate was not affected significantly by the modification of the Asp^{641}, as indicated by the moderate change in the K_s value for the enzyme variant (Table III). The similar binding is also consistent with the crystal structure of the enzyme·substrate complex, which is practically the same as the corresponding complex formed with the wild-type enzyme. In the complex formed with the alanine variant, stabilization of the imidazole ring, in contrast with the Asp^{641} or Asn^{641} variants, is not possible by an amino acid residue, yet the ring assumes the same position as in the wild-type enzyme. This does not support the idea that the large reduction in k_{cat}/K_m arises from the incompetent tautomer of His^{680}.

A further insight into the binding mode has been obtained from the ΔF_{max}, which displays comparable values for the binding and the total hydrolysis of the octapeptide measured under identical experimental conditions. This shows that the internal fluorescence quenching in the substrate is eliminated upon binding to the S554A variant. Surprisingly, the ΔF_{max} is much less in the complex of the S554A/D641A variant, which indicates that considerable alteration in the energy transfer between donor and acceptor groups is still present. The similar crystal structures of the two complexes cannot account for this difference.

To properly function, only the histidine tautomer that is deprotonated at Nϵ2 is catalytically active (Fig. 6*A*). The D102N mutation in trypsin resulted in the incorrect tautomer

[1] The abbreviation used is: r.m.s., root mean square.

form (Fig. 6*B*). In contrast, the D641N mutant of prolyl oligopeptidase underwent structural perturbation, which resulted in retention of the correct tautomer of the catalytic histidine (Fig. 6*C*). This is supported by the fact that Asn^{641} is pushed out of hydrogen bonding range from Nδ1 of His^{680} to a van der Waals distance; *i.e.* Nδ1 cannot act as a proton acceptor.

In the wild-type trypsin structure His^{57} is in an energetically unfavorable conformation (*gauche* +). When it gets double protonated at lower pH, it swings out to a more favorable *trans* position (12). This was presumably partially because of steric repulsion between Nδ2 of Asn^{102} and the protonated Nδ1 of His^{57}. It should be noted that His^{680} of prolyl oligopeptidase is already in the favorable *trans* conformation ($\chi1 = -150°$, $-154°$ in the wild-type) and would be less likely to undergo a similar structural change. The *gauche* − ($\chi1 \sim -60°$) conformation is energetically more favorable, but would result in steric clashes of His^{680} with the main-chain of Asp^{642}. The *gauche* + ($\chi1 \sim 60°$) conformation is adoptable for His^{680} (solvent region in the cavity) but is highly unfavorable.

Although our crystal structure determination argues for similar positions of the imidazole ring in the wild-type and the modified enzymes, the different binding constants of the product-like inhibitor, Z-Gly-Pro-OH (Table IV), are apparently inconsistent with an unchanging imidazole ring. Indeed, a large difference is observed below pH 6 (Fig. 4), where the histidine becomes double protonated, and structural data are not available, because proper crystals could not be obtained at low pH. Thus, some movement of the imidazole ring, which precludes the inhibitor binding as in the wild-type enzyme, cannot be excluded.

The similar catalytic properties of the D641N and D641A variants of prolyl oligopeptidase point to the value of the negative charge of Asp^{641} and discount the catalytic significance of an incompetent tautomer of the active site histidine. This is consistent with the earlier suggestion that a major function of the aspartate residue is to stabilize the transition state on the way to the ion-pair formed with the tetrahedral intermediate and the imidazolium ion (2, 7). The cleavage of a stronger bond involves a transition state of higher energy; therefore, the contribution of the negative charge is less effective in the case of a weaker bond, like that of an ester. This is supported by the present finding with substrates possessing various leaving groups. Interestingly, this effect was not observed in trypsin catalysis, where the reactions were carried out within a more restricted range of bond strength.

Acknowledgments—We thank I. Szamosi and the late J. Fejes for excellent technical assistance. D. R. thanks the Biotechnology and Biological Sciences Research Council for the award of a studentship. We are grateful for access and user support to the synchrotron facilities of European Synchrotron Radiation Facility (Grenoble, France) and Synchrotron Radiation Source (Daresbury, UK).

REFERENCES

1. Blow, D. M., Birktoft, J. J., and Hartley, B. S. (1969) *Nature* **221,** 337–340
2. Polgár, L., and Bender, M. L. (1969) *Proc. Natl. Acad. Sci. U. S. A.* **64,** 1335–1342
3. Bachovchin, W. W., and Roberts, J. D. (1978) *J. Am. Chem. Soc.* **100,** 8041–8047
4. Bachovchin, W. W., Kaiser, R., Richards, J. A., and Roberts, J. D. (1981) *Proc. Natl. Acad. Sci. U. S. A.* **78,** 7323–7326
5. Jordan F., and Polgár, L. (1981) *Biochemistry* **20,** 6366–6370
6. Kossiakoff, A. A., and Spencer, S. A. (1981) *Biochemistry* **20,** 6462–6474
7. Polgár, L. (1972) *Acta Biochim. Biophys. Acad. Sci. Hung.* **7,** 29–34
8. Fersht, A. R., and Sperling, J. (1973) *J. Mol. Biol.* **74,** 137–149
9. Warshel, A. (1978) *Proc. Natl. Acad. Sci. U. S. A.* **75,** 5250–5254
10. Polgár, L. (1989) *Mechanisms of Protease Action*, pp. 87–122, CRC Press, Inc., Boca Raton, FL
11. Polgár, L. (1987) *New Compr. Biochem.* **16,** 159–200
12. Sprang, S., Standing, T., Fletterick, R. J., Stroud, R. M., Finer-Moore, J., Xuong, N-H., Hamlin, R., Rutter, W. J., and Craik, C. C. (1987) *Science* **237,** 905–909
13. Craik, C. S., Roczniak, S., Largman, C., and Rutter, W. J. (1987) *Science* **237,** 909–913
14. Rennex, D., Hemmings, B. A., Hofsteenge, J., and Stone, S. R. (1991) *Biochemistry* **30,** 2195–2203
15. Rawlings, N. D., Polgár, L., and Barrett, A. J. (1991) *Biochem. J.* **279,** 907–911
16. Polgár, L. (1994) *Methods Enzymol.* **244,** 188–200
17. Polgár, L. (2002) Cell. *Mol. Life Sci.* **59,** 349–362
18. Wilk, S. (1983) *Life Sci.* **33,** 2149–2157
19. Mentlein, R. (1988) *FEBS Lett.* **234,** 251–2566
20. Cunningham, D. F., and O'Connor, B. (1997) *Biochim. Biophys. Acta* **1343,** 160–186
21. Yoshimoto, T., Orlowski, C. R., and Walter, R. (1977) *Biochemistry* **16,** 660–665
22. Atack, J. R., Suman-Chauhan, N., Dawson, G., and Kulagowski, J. J. (1991) *Eur. J. Pharmacol.* **205,** 157–163
23. Miura, N., Shibata, S., and Watanabe, S. (1995) *Neurosci. Lett.* **196,** 128–130
24. Portevin, B., Benoist, A., Rémond, G., Hervé, Y., Vincent, M., Lepagnol, J., and De Nanteuil, G. (1996) *J. Med. Chem.* **39,** 2379–2391
25. Maes, M., Goossens, F., Scharpé, S., Meltzer, H. Y., D'Hondt, P., and Cosyns, P. (1994) *Biol. Psychiatry* **35,** 545–552
26. Williams, R. S. B., Eames, M., Ryves, W. J., Viggars, J., and Harwood, A. J. (1999) *EMBO J.* **18,** 2734–2745
27. Welches, W. R., Brosnihan, K. B., and Ferrario, C. M. (1993) *Life Sci.* **52,** 1461–1480
28. Fülöp, V., Böcskei, Z., and Polgár, L. (1998) *Cell* **94,** 161–170
29. Fülöp, V., Szeltner, Z., and Polgár, L. (2000) *EMBO Rep.* **1,** 277–281
30. Szeltner, Z., Renner, V., and Polgár, L. (2000) *Protein Sci.* **9,** 353–360
31. Leatherbarrow, R. J. (2001) *GraFit*, Version 5, Erythacus Software Ltd., Staines, Middlesex, United Kingdom
32. Cornish-Bowden, A. (1995) *Fundamentals of Enzyme Kinetics*, pp. 44–47, Portland Press Ltd., London, United Kingdom
33. Polgár, L. (1999) *Proteolytic Enzymes. Tools and Targets*, pp. 148–166, Springer-Verlag, Berlin
34. Segel, I. H. (1975) *Enzyme Kinetics*, pp. 72–74, John Wiley & Sons, Inc., New York
35. Shaw, E., and Green, D. J. (1981) *Methods Enzymol.* **80,** 820–826
36. Kettner, C., and Shaw, E. (1981) *Methods Enzymol.* **80,** 827–843
37. Tian, W-X., and Tsou, C-L. (1982) *Biochemistry* **21,** 1028–1032
38. Tsou, C-L. (1988) *Adv. Enzymol. Relat. Areas Mol. Biol.* **61,** 381–436
39. Otwinowski, Z., and Minor, W. (1997) *Methods Enzymol.* **276,** 307–326
40. Brünger, A. T. (1992) *X-PLOR*, Version 3.1, Yale University Press, New Haven, CT
41. Jones, T. A., Zou, J. Y., Cowan, S. W., and Kjeldgaard, M. (1991) *Acta Crystallogr. Sect. A* **47,** 110–112
42. Polgár, L. (1995) *Biochem. J.* **312,** 267–271
43. Carter, P., and Wells, J. A. (1988) *Nature* **332,** 564–568
44. Polgár, L. (1992) *Biochem. J.* **283,** 647–648
45. Polgár, L., Kollát, E., and Hollósi, M. (1993) *FEBS Lett.* **322,** 227–230
46. Kirschke, H., and Wiederanders, B. (1999) *Proteolytic Enzymes. Tools and Targets*, pp. 11–28, Springer-Verlag, Berlin
47. Fülöp, V., Szeltner, Z., Renner, V., and Polgár, L. (2001) *J. Biol. Chem.* **276,** 1262–1266
48. Szeltner, Z., Renner, V., and Polgár, L. (2000) *J. Biol. Chem.* **275,** 15000–15005
49. Stone, S. R., Rennex, D., Wikstrom, P., Shaw, E., and Hofsteenge, J. (1991) *Biochem. J.* **276,** 837–840
50. Read, R. J. (1986) *Acta Crystallogr. Sect. A* **42,** 140–149
51. Kraulis, P. J. (1991) *J. Appl. Crystallogr.* **24,** 946–950
52. Esnouf, R. M. (1997) *J. Mol. Graphics* **15,** 133–138
53. Brünger, A. T. (1992) *Nature* **355,** 472–474